Wind and Structures, Vol. 16, No. 1 (2013) 61-91
DOI: http://dx.doi.org/10.12989/was.2013.16.1.061

Internal pressure dynamics of a leaky and quasi-statically flexible building with a dominant opening

T.K. Guha*, R.N. Sharma and P.J. Richards

Department of Mechanical Engineering, The University of Auckland, Private Bag 92019, Auckland, New Zealand

(Received December 27, 2010, Revised October 10, 2011, Accepted November 28, 2011)

Abstract. An analytical model of internal pressure response of a leaky and quasi-statically flexible building with a dominant opening is provided by including the effect of the envelope external pressure fluctuations on the roof, in addition to the fluctuating external pressure at the dominant opening. Wind tunnel experiments involving a flexible roof and different building porosities were carried out to validate the analytical predictions. While the effect of envelope flexibility is shown to lower the Helmholtz frequency of the building volume-opening combination, the lowering of the resonant peak in the internal and net roof pressure coefficient spectra is attributed to the increased damping in the system due to inherent background leakage and envelope flexibility. The extent of the damping effects of "skin" flexibility and background leakage in moderating the internal and net pressure response under high wind conditions is quantified using the linearized admittance functions developed. Analytical examples provided for different combinations of background leakage and envelope flexibility show that alleviation of internal and net pressure fluctuations due to these factors by as much as 40 and 15% respectively is possible compared to that for a nominally sealed rigid building of the same internal volume and opening size.

Keywords: internal pressure; leaky; quasi-statically flexible; building; dominant opening; wind tunnel experiments; helmholtz frequency; net roof pressure; admittance function

1. Introduction

The importance of wind induced internal pressure in the safety of building components and claddings in cyclone prone areas cannot be stressed enough. The net load generated on the building envelope as a result of the combination of external pressure and internal pressure established through an opening either left open accidentally or created by the impact of debris can far exceed the design value resulting in catastrophic failure. A number of wind tunnel studies (for example Oh *et al*. 2007) have corroborated this view and highlighted the need for further strengthening of the quasi-steady based provisions of internal pressure in current wind loading standards. While the merits and contribution of these studies in comprehending the underlying physics of internal pressure cannot be denied, the reluctance of the code committees in implementing their suggestions stems from the idealizations involved in these experiments such as the usage of non-leaky rigid walled building models not representative of real buildings.

*Corresponding author, Graduate student, E-mail: tguh001@aucklanduni.ac.nz

Several of these early studies (e.g., Sharma and Richards 2003, 2005, Woods and Blackmore 1995) did not use volume scaling, which as stated by Holmes (1979) is necessary to maintain the dynamic similarity between model and full scale. As such the applicability of the vigorous and pronounced Helmholtz resonance of internal pressure reported by these studies appears questionable in real buildings of any appreciable size and volume. While full scale studies of internal pressure carried out for a range of opening sizes and building volumes with intrinsic background leakage and flexibility under design wind conditions offer the best prospect for getting a realistic picture of the problem and to ascertain the need for modifications, if any, in the wind loading provisions, such studies are difficult in practice and often very resource intensive, time consuming and expensive. Analytical models of internal pressure dynamic response parameterized using full scale, wind tunnel and/or computational fluid dynamics (CFD) studies on the other hand, have been known to perform satisfactorily in predicting the severity of internal pressure as well as providing design solutions of internal pressure in practice.

The first authentic model of wind-induced internal pressure dynamics of a rigid non-leaky building with a single dominant opening supported by experiments was provided by Holmes (1979) who used an acoustic resonator based analogy to show the possibility of occurrence of strong internal pressure resonance. The stiffness of the air-slug oscillating through the opening as shown in Fig. 1 is considered to have been provided by the internal volume of air acting as a pneumatic spring and damped by the irrecoverable energy lost due to flow past the opening.

The model was subsequently modified by Liu and Saathoff (1982) using a fluid mechanics approach based on the unsteady Bernoulli's equation with isentropic density formulation, for flow past a sharp edged orifice, although a difference of opinion regarding the presence of a discharge coefficient in the inertia term exists. Vickery (1991) attributed this discrepancy to the definition of the effective length adopted by Liu and Saathoff (1982) being different from the commonly accepted expression offered by potential flow theory. He argued that the flow conditions through the opening will essentially be unsteady and attached and any mismatch between the observed and predicted Helmholtz frequency should be attributed to the deviation in the value of the effective length from its ideal potential flow situation. Vickery and Bloxham (1992), and later Sharma and Richards (1997a), made minor modifications to the analytical model based on heuristic arguments and CFD flow visualization respectively with regard to the usage of the ill-defined parameters namely, discharge coefficient, loss coefficient and the effective air-slug length in the equation.

More recently, Ginger *et al.* (2008, 2010) and Holmes and Ginger (2012) provided design solutions of the non-dimensional governing equation proposed by Holmes (1979) for a range of building volume and opening sizes. In particular, the numerically (Ginger *et al.* 2008) and analytically (Ginger *et al.* 2010) obtained non-dimensional design solutions were compared to full scale data and wind tunnel data respectively. An empirical non-dimensional design solution that provided a better fit to the experimental data was also proposed (Holmes and Ginger 2012).

Some insights into the effect of envelope flexibility on the dynamics of internal pressure in the presence of a dominant opening was provided by the analytical study of Vickery (1986), in which the building structure was considered to respond in a quasi-static manner with deflections being assumed to be proportional to the applied load at all times. The theoretical studies of Novak and Kaseem (1990) and Vickery and Georgiou (1991) directed at large span self- or air supported structures such as stadia or sport arenas have attempted to describe the interaction between a flexible roof backed by a cavity with openings as simple two degree of freedom systems. While the first of these studies validated the theoretical predictions of Helmholtz frequency and damping ratios with experimental tests on scaled models in still air, Vickery and Georgiou (1991)

considered the effect of opening to roof area ratio on the form of transfer function and root-mean-squared values of fluctuating roof response with zero roof damping. Sharma and Richards (1997b) and Sharma (2008) presented analytical models of the characteristics of internal pressure response of flexible roofed low rise buildings in the presence of dominant openings by including the effect of roof damping. The assumption of a quasi-statically flexible envelope is shown to be a special case of the general dynamic model presented in the first study which did not however include the influence of fluctuating external and hence net pressure on the building envelope. The second study included the characteristics of fluctuating external pressure in influencing the internal and the net pressure on the building with quasi-statically flexible envelope.

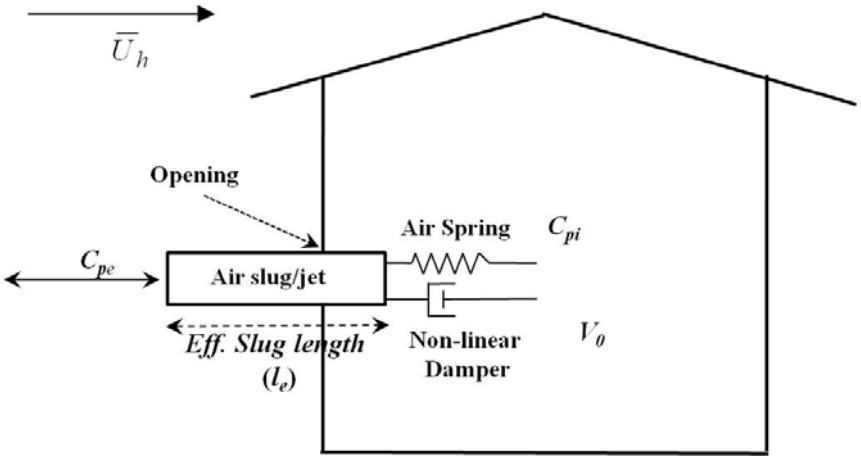

Fig.1 Air slug model (Holmes 1979)

In theoretical treatments of the internal pressure response of a nominally-sealed building, with uniformly distributed background leakage, as reported by Vickery (1986) and Harris (1990), the leakages were lumped into two equivalent openings on the windward and leeward wall respectively. The effect of inertia through leakages is shown to be negligible in comparison to the magnitude of damping and thus neglected in the development of their non-linear models. A characteristic frequency (ω_c) based on the characteristic relaxation time constant (T_c=1/ω_c) of the lumped leakage area - building volume combination derived by linearizing the model is shown to act as a low pass filter attenuating high frequency fluctuations through the leakage path. Wind tunnel and numerical studies of internal pressure on a 1:100 scale building model in open and suburban terrain with two different dominant opening sizes and well-defined uniformly distributed background leakage were reported by Oh *et al.* (2007). The multiple discharge equation (MDE) approach that involves simultaneous solution of the equations of motion through individual openings (both dominant openings and leakages) was found to provide the best agreement with the experimental results, especially for buildings with porosity ratios greater than 10%. Yu *et al.* (2008) proposed a non-linear model of internal pressure response, for a building with a dominant opening and background leakage based on the lumped-leakage concept, by neglecting the effect of inertia in flow through the leakages. The theoretical predictions were supported by experimental evidence.

Thus, it appears from a review of the state of the art that, while analytical models to account for the effect of envelope flexibility and background leakage on internal pressure dynamics exist separately, no attempt to develop a unified model by including the effect of both envelope

flexibility and leakage, as occurs in most real buildings, has been made to date. It is the purpose of this paper to address the outstanding issues of the characteristics of internal pressure in such buildings using an analytical approach, due to the recognized practical difficulty in similarity based wind-tunnel modeling of such a "realistic" scenario. The influence of envelope external pressure fluctuations on the roof, in addition to the fluctuating external pressure at the dominant opening, for leaky buildings with quasi-statically flexible envelope have been considered in the current study. Wind-tunnel experiments involving a flexible roof and different building porosities were carried out to validate the analytical predictions. In particular, the extent of the damping effects of "skin" flexibility and background leakage in moderating the internal pressure response of buildings with a dominant opening is numerically investigated. This exercise is extremely relevant in determining the significance of internal pressure as a design parameter, and the adequacy of the provisions in current wind loading codes and standards as a whole.

2. Governing equations

The model developed here is an extension of the flexibility model of Sharma (1996) to include the additional effects of background leakage.

2.1 The general case

The general problem considered here is the response of internal pressure to fluctuating external pressure in a building with a windward dominant opening, flexible envelope and background leakage.

In particular, the flexibility of the envelope is considered to be concentrated at the roof, a common feature with most buildings especially in the tropics, such that the internal air volume changes under the action of both internal and roof external pressure fluctuations. A significant approximation in the model is the usage of a rigid body with uniform deflection to represent a flexible roof; contrary to real roofs being continuous dynamic systems having variable static and dynamic deflections over its area.

The leakages are lumped onto the leeward side because of the relative insensitivity of the leakages to their location on the building wall due to their apparent quasi-steady nature. Leakages lumped onto other walls with suction pressure will produce a similar dynamic response of internal pressure. Fig. 2 presents a schematic of the proposed model.

Conservation of mass requires the difference in the rate of mass influx and efflux at the opening to be equal to the rate of change of mass of air inside the building cavity as

$$\frac{\rho_a c A_W \dot{x}_W - \rho_a A_L \dot{x}_L}{V_0} = \rho_a \frac{d\upsilon}{dt} + \upsilon \frac{d\rho_a}{dt} \tag{1}$$

where ρ_a, c and A_W are the density of air, flow contraction coefficient and area of the windward dominant opening respectively, A_L and V_o are the area of the lumped leakage and the nominal volume of the building envelope respectively, $\dot{x}_W$ and $\dot{x}_L$ are the velocities of air jet through the windward dominant opening and lumped leakage respectively. The non-dimensional volume ratio, υ, and its time derivatives are given as

$$\upsilon = \frac{V}{V_o} = \frac{A_r\left(H_r + x_r\right)}{A_r H_r} = 1 + \frac{x_r}{H_r}$$
$$\dot{\upsilon} = \frac{\dot{x}_r}{H_r}$$
$$\ddot{\upsilon} = \frac{\ddot{x}_r}{H_r} \tag{2}$$

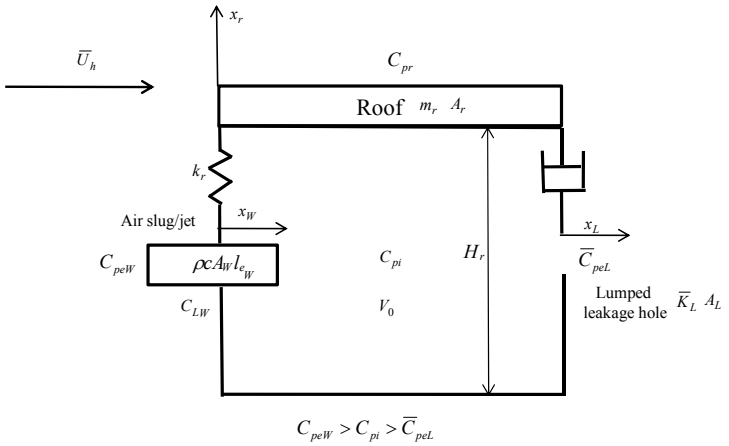

Fig. 2 Schematic of the proposed theoretical model

where V and H_r are the instantaneous volume and ridge height of the building envelope respectively, A_r is the area of the roof and x_r, $\dot{x}_r$, $\ddot{x}_r$ is the instantaneous roof displacement, velocity and acceleration respectively.

Assuming air density changes to be small, the unsteady form of Bernoulli's equation through the windward dominant opening applied to a streamline connecting the immediate external region, with external pressure coefficient $C_{peW}(t)$, to an internal point within the convergent flow region with pressure coefficient $C_{pi}(t)$, can be written as

$$\rho_a l'_{eW} c A_W \ddot{x}_W + \frac{1}{2}\rho_a C_{LW} c A_W \left|\dot{x}_W\right| \dot{x}_W = c A_W q\left(C_{peW} - C_{pi}\right) \tag{3}$$

where l'_{eW} and $\ddot{x}_W$ are the effective length and acceleration of the air slug through the windward dominant opening respectively, C_{LW} is the loss coefficient of flow through the opening and q=0.5$\rho_a \overline{U}_h^2$ is the reference ridge height dynamic pressure. The effective air slug length (l'_{eW}) has a standard value of $\sqrt{\pi A_W / 4}$ from potential flow considerations, however for inverse oscillating flows superimposed on mean flow type conditions considered here, the effective slug

length will vary considerably along with the flow contraction coefficient (c). Hence, as proposed by Vickery (1994), it is preferable to quantify the net effective slug length (l_{eW}) in terms of an inertia coefficient (C_I) by combining together all the ill-defined terms. The net effective air slug length has thus been formulated as $l_{eW} = C_I\sqrt{A_W} = l'_{eW}/c = \sqrt{\pi/4}\sqrt{A_W}/c$ in this study, in which a match between the theoretical and measured Helmholtz frequency can be obtained by choosing an appropriate value of c.

The quasi-steady equation of motion through the lumped leakage opening obtained by neglecting the effect of inertia is written as

$$\frac{\rho_a}{2}\overline{K}_L\dot{x}_L|\dot{x}_L| = q\left(C_{pi} - \overline{C}_{peL}\right) \tag{4}$$

where $\overline{C}_{peL}$ is the spatio-temporal average of leeward pressure over the lumped leakage opening (Yu *et al*. 2008) and $\overline{K}_L$ is the equivalent loss coefficient through the lumped leakage opening under steady state condition which may be grossly estimated using the Bernoulli's obstruction theory (White 1999) as

$$\overline{K}_L = \frac{1-\phi_L^2}{\left(c'_d\right)^2} \tag{5}$$

where c'_d is the discharge coefficient of flow through the lumped leeward opening and porosity ϕ_L may be taken as the ratio of the lumped leakage (A_L) to the leeward wall area ($A_{Leewall}$) i.e.

$$\phi_L = A_L/A_{Leewall} \tag{6}$$

It is reasonable to assume for all practical purposes that $A_L << A_{Leewall}$, so that Eq. (5) can be further simplified to

$$\overline{K}_L \approx 1/\left(c'_d\right)^2 \tag{7}$$

Invoking the isentropic pressure-volume relationship of air, along with Eqs. (1), (3) and (4), leads to the generalized governing equation of the internal pressure response of leaky and dynamically flexible buildings (see the Appendix for a complete derivation) with a dominant opening for $\upsilon \approx 1$ as

$$\underbrace{\frac{V_0\rho_a l_{eW}}{\gamma P_a A_W}\ddot{C}_{pi}}_{\text{Intertial Term}} + \underbrace{\frac{V_0\rho_a l_{eW}}{\gamma P_a A_W}\dot{\upsilon}\dot{C}_{pi}}_{\text{Interaction Damping Term}} + \underbrace{\frac{l_{eW}}{\overline{U}_h\sqrt{\overline{K}_L}}\left(\frac{A_L}{A_W}\right)\frac{\dot{C}_{pi}}{\sqrt{\left(C_{pi}-\overline{C}_{peL}\right)}}}_{\text{Pseudo-linear Damping Term}} + \frac{V_0\rho_a l_{eW}}{qA_W}\ddot{\upsilon}$$

$$+ \underbrace{C_{LW}\frac{V_0^2\rho_a q}{2\left(\gamma P_a A_W\right)^2}\left|\dot{C}_{pi}+\frac{2A_L\gamma P_a}{\rho_a\overline{U}_h V_0\sqrt{\overline{K}_L}}\left[\left(C_{pi}-\overline{C}_{peL}\right)\right]^{1/2}+\frac{\gamma P_a}{q}\dot{\upsilon}\right|\left(\dot{C}_{pi}+\frac{2A_L\gamma P_a}{\rho_a\overline{U}_h V_0\sqrt{\overline{K}_L}}\left[\left(C_{pi}-\overline{C}_{peL}\right)\right]^{1/2}+\frac{\gamma P_a}{q}\dot{\upsilon}\right)}_{\text{Non-linear Damping Term}} \tag{8}$$

$$= \underbrace{C_{peW}}_{\text{Forcing Function}} - \underbrace{C_{pi}}_{\text{Stiffness Term}}$$

The additional terms namely the interaction damping term and the pseudo-linear damping term in Eq. (8), due to the inclusion of the effects of envelope flexibility and background leakage respectively, can be seen to impart additional damping into the internal pressure response. This is in addition to the non-linear damping term, further augmented by interaction with envelope flexibility and background porosity, which can further limit the magnitude of internal pressure fluctuations at resonance in real buildings. For a rigid and non-leaky building, Eq. (8) can be simplified by substituting $\upsilon=\dot{\upsilon}=\ddot{\upsilon}=0$ and $A_L=0$ so that the well-known governing equation of internal pressure dynamics for a single cavity, rigid, non-porous building as originally proposed by Holmes (1979) is obtained.

The dynamic equation of motion of the flexible roof (Sharma and Richards 1997b) assuming it to be a mass-spring-damper system is given by

$$\ddot{x}_r = \frac{qA_r}{m_r}\left(C_{pi}-C_{pr}\right)-\omega_r^2 x_r - 2\omega_r\zeta_r\dot{x}_r$$
$$\omega_r^2 = \frac{k_r}{m_r} \tag{9}$$

where k_r, ζ_r and ω_r are the structural stiffness, damping ratio and structural frequency of the roof respectively and $C_{pr}(t)$ is the fluctuating roof external pressure coefficient. Using Eqs. (2) and (9) can be re-written as

$$\ddot{\upsilon} = \frac{qA_r^2}{m_r V_o}\left(C_{pi}-C_{pr}\right)-\omega_r^2\left(\upsilon-1\right)-2\omega_r\zeta_r\dot{\upsilon} \tag{10}$$

which, together with Eq. (8), can be used to solve simultaneously the internal pressure and roof response characteristics concurrently, when forced by fluctuating roof external and opening external pressure coefficients.

2.2 *Quasi-static structural response*

When the structural frequency of the building components such as the roof in the current study is considerably higher than the frequencies over the energy containing region of the onset wind turbulence, the structure will respond almost quasi-statically to the applied loading. The instantaneous roof displacement is assumed to be linearly proportional to the applied loading and can be expressed using Eqs. (2) and (10) as

$$\begin{aligned} \upsilon &= \frac{V}{V_o} = \frac{q\left(C_{pi} - C_{pr}\right)}{K_B} + 1 \\ \dot{\upsilon} &= \frac{q}{K_B}\left(\dot{C}_{pi} - \dot{C}_{pr}\right) \\ \ddot{\upsilon} &= \frac{q}{K_B}\left(\ddot{C}_{pi} - \ddot{C}_{pr}\right) \end{aligned} \tag{11}$$

where K_B is the bulk modulus of the building. Substituting Eq. (11) in Eq. (8) leads to

$$\begin{aligned} &\frac{V_0(1+b)\rho_a l_{eW}}{\gamma P_a A_W}\left(\ddot{C}_{pi} - \frac{b}{1+b}\ddot{C}_{pr}\right) + \frac{l_{eW}}{\overline{U}_h\sqrt{\overline{K}_L}}\left(\frac{A_L}{A_W}\right)\frac{\dot{C}_{pi}}{\sqrt{\left(C_{pi} - \overline{C}_{peL}\right)}} \\ &+ C_{LW}\frac{V_0^2(1+b)^2\rho_a q}{2\left(\gamma P_a A_W\right)^2}\left|\dot{C}_{pi} - \frac{b}{1+b}\dot{C}_{pr} + \frac{2A_L\gamma P_a}{\rho_a\overline{U}_h V_0(1+b)\sqrt{\overline{K}_L}}\left[\left(C_{pi} - \overline{C}_{peL}\right)\right]^{1/2}\right| \\ &\left(\dot{C}_{pi} - \frac{b}{1+b}\dot{C}_{pr} + \frac{2A_L\gamma P_a}{\rho_a\overline{U}_h V_0(1+b)\sqrt{\overline{K}_L}}\left[\left(C_{pi} - \overline{C}_{peL}\right)\right]^{1/2}\right) \\ &= C_{peW} - C_{pi} \end{aligned} \tag{12}$$

where b is the ratio of the bulk modulus of air to that of the building

$$b = \frac{\gamma P_a}{K_B} \tag{13}$$

This is estimated to vary between 0.2 for stiff structures to 5.0 for flexible large span roof structures as per Vickery (1986). Eq. (12) describes the response of internal pressure of a building with leaky envelope when the roof structure responds in a quasi-static manner and is thus a special case of the more generalized model represented by Eq. (8). The undamped Helmholtz frequency $f'_{HH} = \omega'_{HH}/2\pi$ is readily obtained from Eq. (12) as

$$f'_{HH} = \frac{\omega'_{HH}}{2\pi} = \frac{1}{2\pi}\sqrt{\frac{\gamma P_a A_W}{V_0(1+b)\rho_a l_{eW}}} = \frac{1}{2\pi}\sqrt{\frac{\gamma P_a A_W}{V_0 \rho_a l_{eW}}}\sqrt{\frac{1}{(1+b)}} = \frac{f_{HH}}{\sqrt{(1+b)}} \tag{14}$$

can be shown to have been reduced by the presence of "skin" flexibility in comparison to that for a rigid building (f_{HH}).

2.3 *Linearized model*

A linearized internal pressure system consisting of a windward dominant opening, a lumped leeward leakage and a quasi-statically flexible roof represented by Fig. 2 will essentially involve linearizing the non-linear Eqs. (3) and (4) with appropriate simplifications. The linearized versions of the equation of motion of the air slug through the dominant windward opening, under the assumption of Gaussian distribution of internal pressure and the lumped leakage linearized about its mean, are given by

$$\rho_a l_{eW}\ddot{x}_W + c_{j1}\dot{x}_W = q\left(C_{peW} - C_{pi}\right) \tag{15a}$$

$$\rho_a \frac{\overline{Q}_L}{A_L}\sqrt{\left|\overline{C}_{pi} - \overline{C}_{peL}\right|}\sqrt{\overline{K}_L}\,\dot{x}_L = q\left(C_{pi}\right) \tag{15b}$$

where c_{j1} is the damping coefficient per unit area of flow past the dominant opening, $\overline{Q}_L$ is the mean flow rate through the lumped leeward opening, and $\overline{C}_{pi}$ is the mean internal pressure coefficient. Eq. (15) in combination with Eqs. (1) and (11) lead to the linearized version of the model as

$$\begin{aligned}&\frac{V_0(1+b)\rho_a l_{eW}}{\gamma P_a A_W}\left(\ddot{C}_{pi} - \frac{b}{1+b}\ddot{C}_{pr}\right) + \frac{\rho_a l_{eW}}{\left[\rho_a \overline{U}\sqrt{\left|\overline{C}_{pi} - \overline{C}_{peL}\right|}\sqrt{\overline{K}_L}\right]}\left(\frac{A_L}{A_W}\right)\dot{C}_{pi}\\ &+ c_{j1}\left[\frac{V_o(1+b)}{A_W \gamma P_a}\left(\dot{C}_{pi} - \frac{b}{1+b}\dot{C}_{pr}\right) + \frac{A_L}{A_W\left[\rho_a \overline{U}\sqrt{\left|\overline{C}_{pi} - \overline{C}_{peL}\right|}\sqrt{\overline{K}_L}\right]}C_{pi}\right] = C_{peW} - C_{pi}\end{aligned} \tag{16}$$

where c_{j1} can be determined following the work of Vickery and Bloxham (1992) as

$$c_{j1}=\sqrt{\frac{8}{\pi}}\frac{C_{LW}\rho_a q}{2}\left[\begin{array}{l}\left(\dfrac{V_o(1+b)}{\rho_a l_{eW}A_W\gamma P_a}\right)\left(\widetilde{C}_{pi}^2+\dfrac{b^2}{(1+b)^2}\widetilde{C}_{pr}^2-2\dfrac{b}{(1+b)}\rho_{ir}\widetilde{C}_{pi}\widetilde{C}_{pr}\right)\\ +\left(\dfrac{A_L}{A_W\left[\rho_a\overline{U}\sqrt{\left|\overline{C}_{pi}-\overline{C}_{peL}\right|}\sqrt{\overline{K}_L}\right]}\right)^2\left(\widetilde{C}_{pi}\right)^2\\ -2\dfrac{b}{(1+b)}\dfrac{A_L}{\overline{U}}\sqrt{\dfrac{V_o(1+b)}{\rho_a l_{eW}\gamma P_a A_W\overline{K}_L\left(\left|\overline{C}_{pi}-\overline{C}_{peL}\right|\right)}}\rho_{ir}\widetilde{C}_{pi}\widetilde{C}_{pr}\end{array}\right]^{1/2} \tag{17}$$

where ρ_{ir} is the correlation coefficient between the fluctuating internal and roof external pressures.

Assuming $\overline{C}_{pi}\approx\overline{C}_{peW}$ for a building with a dominant opening, i.e., the internal pressure inside the building approximates to a value close to the mean external pressure over the dominant opening, the critical leakage frequency (ω_c), in radians/s, above which external pressure fluctuations are attenuated and not passed effectively through the lumped leakage opening can be defined as

$$\omega_c=\frac{A_L\gamma P_a}{\rho_a\overline{U}V_o(1+b)\sqrt{\overline{K}_L}\sqrt{\overline{C}_{pi}-\overline{C}_{peL}}}\approx\frac{A_L\gamma P_a}{\rho_a\overline{U}V_o(1+b)\sqrt{\overline{K}_L}\sqrt{\overline{C}_{peW}-\overline{C}_{peL}}} \tag{18}$$

Eqs. (14) and (18) can be used to re-cast Eqs. (16) and (17) in a more familiar form as

$$\begin{aligned}&\underbrace{\frac{1}{\omega_{HH}'^2}\left(\ddot{C}_{pi}-\frac{b}{1+b}\ddot{C}_{pr}\right)}_{\text{Inertial term}}+\underbrace{\left(\frac{\omega_c}{\omega_{HH}'^2}\right)\dot{C}_{pi}}_{\text{Damping term 1}}\\ &C_{LW}\frac{\sqrt{8\pi}V_o^2(1+b)^2\rho_a q f_{HH}'}{\left(A_W\gamma P_a\right)^2}\\ &+\left[\left\{1+\left(\frac{\omega_c}{\omega_{HH}'}\right)^2\right\}\widetilde{C}_{pi}^2+\left(\frac{b}{1+b}\right)^2\widetilde{C}_{pr}^2-2\rho_{ir}\frac{b}{1+b}\left(1+\frac{\omega_c}{\omega_{HH}'}\right)\widetilde{C}_{pi}\widetilde{C}_{pr}\right]^{\frac{1}{2}}\\ &\underbrace{\left[\left(\dot{C}_{pi}-\frac{b}{1+b}\dot{C}_{pr}\right)+(\omega_c)C_{pi}\right]}_{\text{Damping term 2}}\\ &+\underbrace{C_{pi}}_{\text{Stiffness term}}=\underbrace{C_{peW}}_{\text{Foricng function}}\end{aligned} \tag{19}$$

$$c_{j1} = \sqrt{8\pi}\,\frac{C_{LW}V_o(1+b)\rho_a q f'_{HH}}{\gamma P_a A_W}\left[\left\{1+\left(\frac{\omega_c}{\omega'_{HH}}\right)^2\right\}\widetilde{C}_{pi}^2+\left(\frac{b}{1+b}\right)^2\widetilde{C}_{pr}^2-2\rho_{ir}\frac{b}{1+b}\left(1+\frac{\omega_c}{\omega'_{HH}}\right)\widetilde{C}_{pi}\widetilde{C}_{pr}\right]^{\frac{1}{2}} \tag{20}$$

The linearized Eq. (19) shows that in addition to the damping caused by energy losses through the dominant opening (given by damping term 2), an additional damping term (damping term 1) proportional to the area of the leakage (or porosity ratio) further contributes to the damping of the internal pressure response for a leaky building with a flexible envelope.

3. Admittance functions

The concept of "admittance" is based on linear systems and input-output assumptions. Although this is strictly not the case with internal pressures, the linearization procedure as described in the previous section has been suitably used to develop frequency dependant admittance functions. The significance of the effects of envelope flexibility and background leakage on the internal pressure dynamics can be understood by examining the admittance functions of fluctuating internal and net roof pressure with respect the onset turbulence in the approach flow i.e. $\left|\chi_{iq}(\omega)\right|^2$ and $\left|\chi_{nq}(\omega)\right|^2$. This however, requires estimation of the admittance functions of internal pressure over opening external ($\left|\chi_{ieW}(\omega)\right|^2$) and roof external ($\left|\chi_{ir}(\omega)\right|^2$) pressures as well as the phase information [$\varphi_{ieW}(\omega)$ and $\varphi_{ir}(\omega)$] obtained by Laplace transforming Eq. (19)

$$\left|\chi_{ieW}(\omega)\right|^2 = \left|\frac{C_{pi}(\omega)}{C_{peW}(\omega)}\right|^2 = \frac{\omega'^4_{HH}}{\left[\left(-\omega^2+\omega'^2_{HH}+\omega_{j1}\omega_c\right)^2+\left(\omega_{j1}\omega+\omega_c\omega\right)^2\right]} \tag{21a}$$

$$\left|\chi_{ir}(\omega)\right|^2 = \left|\frac{C_{pi}(\omega)}{C_{pr}(\omega)}\right|^2 = \left(\frac{b}{1+b}\right)^2\frac{\omega^4+\omega^2\omega_{j1}^2}{\left[\left(-\omega^2+\omega'^2_{HH}+\omega_{j1}\omega_c\right)^2+\left(\omega_{j1}\omega+\omega_c\omega\right)^2\right]} \tag{21b}$$

$$\varphi_{ieW}(\omega) = -\arctan\left(\frac{\omega_{j1}\omega+\omega_c\omega}{-\omega^2+\omega'^2_{HH}+\omega_{j1}\omega_c}\right) \tag{21c}$$

$$\varphi_{ir}(\omega) = \arctan\left(\frac{\omega_{j1}}{\omega}\right)+\varphi_{ieW}(\omega) \tag{21d}$$

where ω_{j1} is defined as follows

$$\omega_{j1} = 2\varsigma_{j1}\omega'_{HH} = \frac{c_{j1}}{\rho_a l_{eW}} = \sqrt{8\pi}\,\frac{C_{LW}V_o(1+b)qf'_{HH}}{\gamma P_a l_{eW} A_W}$$
$$\left[\left\{1+\left(\frac{\omega_c}{\omega'_{HH}}\right)^2\right\}\widetilde{C}_{pi}^2 + \left(\frac{b}{1+b}\right)^2\widetilde{C}_{pr}^2 - 2\rho_{ir}\frac{b}{1+b}\left(1+\frac{\omega_c}{\omega'_{HH}}\right)\widetilde{C}_{pi}\widetilde{C}_{pr}\right]^{\frac{1}{2}} \tag{22}$$

ς_{j1} being the damping ratio in Eq. (22). Eqs. (21) and (22) can be used to derive the final form of the admittance function (Sharma 2008) of fluctuating internal pressure over the ridge height onset turbulence $\left|\chi_{iq}(\omega)\right|^2$ as

$$\left|\chi_{iq}(\omega)\right|^2 = \left(\frac{q}{\overline{C}_{pi}}\right)^2\frac{S_{C_{pi}}(\omega)}{S_q(\omega)} = \left|\chi_{eWq}(\omega)\right|^2\left|\chi_{ieW}(\omega)\right|^2\left(\frac{\overline{C}_{peW}}{\overline{C}_{pi}}\right)^2 + \left|\chi_{rq}(\omega)\right|^2\left|\chi_{ir}(\omega)\right|^2\left(\frac{\overline{C}_{pr}}{\overline{C}_{pi}}\right)^2$$
$$+ 2\left|\chi_{eWq}(\omega)\right|\left|\chi_{ieW}(\omega)\right|\left|\chi_{rq}(\omega)\right|\left|\chi_{ir}(\omega)\right|\left(\frac{\overline{C}_{peW}}{\overline{C}_{pi}}\right)\left(\frac{\overline{C}_{pr}}{\overline{C}_{pi}}\right)\cos(\varphi_{ieW} - \varphi_{ir} + \varphi_{eWr}) \tag{23}$$

where $S_{Cpi}(\omega)$ and $S_q(\omega)$ are the spectra of internal pressure and ridge height dynamic pressures; $\left|\chi_{eWq}(\omega)\right|^2$ and $\left|\chi_{rq}(\omega)\right|^2$ are the admittance functions of windward wall and roof external pressure over the onset turbulence respectively. φ_{eWr} is the phase difference between the opening and roof external pressure fluctuations and $\overline{C}_{peW}$, $\overline{C}_{pr}$ and $\overline{C}_{pi}$ are the mean opening external, roof external and internal pressure coefficients. Of considerable interest, from the point of view of cladding loads, is the magnitude of net pressure on the building roof (C_{pn}) under the combined action of external roof suction (C_{pr}) and the positive internal pressure (C_{pi}) induced through the windward dominant opening. The net roof pressure is estimated as the algebraic difference of the external roof suction and internal pressure i.e., $C_{pn} = C_{pi} \sim C_{pr}$. The admittance function (Sharma 2008) of fluctuating net roof pressure over the ridge height onset turbulence $\left|\chi_{nq}(\omega)\right|^2$ can be expressed as

$$\left|\chi_{nq}(\omega)\right|^2 = \left(\frac{q}{\overline{C}_{pn}}\right)^2\frac{S_{C_{pn}}(\omega)}{S_q(\omega)} = \left|\chi_{eWq}(\omega)\right|^2\left|\chi_{ieW}(\omega)\right|^2\left(\frac{\overline{C}_{peW}}{\overline{C}_{pn}}\right)^2 + \left|\chi_{rq}(\omega)\right|^2\left(\left|\chi_{ir}(\omega)\right|^2+1\right)\left(\frac{\overline{C}_{pr}}{\overline{C}_{pn}}\right)^2$$
$$+ 2\left|\chi_{eWq}(\omega)\right|\left|\chi_{ieW}(\omega)\right|\left|\chi_{rq}(\omega)\right|\left|\chi_{ir}(\omega)\right|\left(\frac{\overline{C}_{peW}}{\overline{C}_{pn}}\right)\left(\frac{\overline{C}_{pr}}{\overline{C}_{pn}}\right)\cos(\varphi_{ieW} - \varphi_{ir} + \varphi_{eWr})$$
$$- 2\left|\chi_{eWq}(\omega)\right|\left|\chi_{ieW}(\omega)\right|\left|\chi_{rq}(\omega)\right|\left(\frac{\overline{C}_{peW}}{\overline{C}_{pn}}\right)\left(\frac{\overline{C}_{pr}}{\overline{C}_{pn}}\right)\cos(\varphi_{ieW} + \varphi_{eWr}) -$$
$$2\left|\chi_{ir}(\omega)\right|\left|\chi_{rq}(\omega)\right|^2\left(\frac{\overline{C}_{pr}}{\overline{C}_{pn}}\right)^2\cos(\varphi_{ir}) \tag{24}$$

where $S_{Cpn}(\omega)$ is the spectra of net roof pressure over the ridge height dynamic pressure and $\overline{C}_{pn}$ is the mean net pressure on the roof. Evaluation of admittance functions $|\chi_{iq}|^2$ and $|\chi_{nq}|^2$ given by Eqs. (23) and (24) however requires the knowledge of opening external and roof pressure admittance functions relative to onset turbulence, $|\chi_{eWq}|^2$ and $|\chi_{rq}|^2$, and also the phase relationship θ_{eWr} between the roof external and opening external pressures. These have been obtained from wind tunnel measurements in the current study.

4. Measurement of admittance and phase functions

Measurement of the admittance and phase functions, $|\chi_{eWq}|^2$, $|\chi_{rq}|^2$ and φ_{eWr}, were carried out for a windward wall opening area of full scale dimensions 5m by 4.2 m, and for a section of the roof (near the windward edge) of dimensions 5 m by 11m using a 1:100 scale wind tunnel acrylic model of the Twisted Flow Wind Tunnel (TFWT) building of the University of Auckland (UoA) as shown in Fig. 3. The Twisted Flow Wind Tunnel (TFWT) building is a typical warehouse consisting of a large hall housing the Twisted Flow Wind Tunnel with adjoining office space. The hall of dimensions 35.1 m by 24.9 m by 7 m consists of a roller door of size 5 m by 4.2 m in its southern wall that opens into a space interspersed with obstructions such as bushes, fences etc. not more than 5 m high. The setting, suburban, in nature is representative of a category 3 terrain profile as per AS/NZS 1170.2.2002 (2002).

A 64 channel pressure measuring system consisting of differential transducers of range ~± 650 Pa (XSCL series, Honeywell Inc.), along with signal conditioning equipment interfaced to a PC through a LABVIEW program, was used for logging the raw voltage data digitized and sampled at 600 Hz. PVC (make Scanivalve) tubings of internal diameter 1.5 mm and length 550 mm were used to transmit the internal, windward and roof external pressure signals to the pressure module, which were subsequently corrected for tubing induced distortion using a time-domain based recursive filter approach (Halkyard *et al.* 2009). Typically data were collected for 120 seconds for each channel for subsequent analysis.

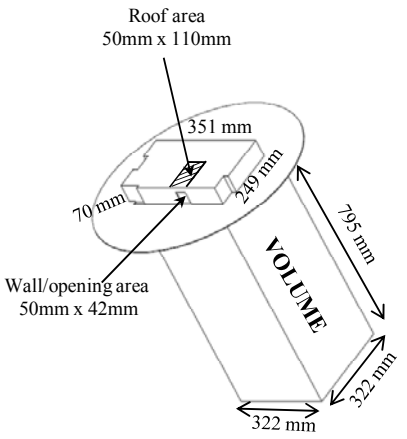

Fig. 3 A 1:100 scale wind tunnel model of the TFWT building with volume scaling

Dynamic similarity between model and full scale necessary for internal pressure measurements, was maintained using volume scaling for a model to full scale velocity ratio of 1:4, for a typical ridge height velocity of 6m/s in the wind tunnel. This was achieved by exaggerating the internal volume of the hall cavity, of dimensions 351 mm by 249 mm by 70 mm, using a sealed plywood chamber 322 mm by 322 mm by 795 mm hanging from the turntable below the tunnel floor as shown in Fig. 3.

The tests were conducted in a boundary layer simulated to terrain category 3, as defined in AS/NZ 1170.2.2002 (2002), in the low speed section of the de Bray wind tunnel of the University of Auckland with test section dimensions of 11 m by 1.8 m by 1.2 m. A combination of turbulence generators including logarithmic spaced grill, vertical spires, saw tooth barrier, floor blocks and gravels of average size 10-20 mm were used to generate the flow. The mean velocity and turbulence intensity profiles of the simulated terrain at the test section centre and at a location 600mm upstream are shown in Figs. 4(a) and (b) along with the target profiles from Australian Standard AS 1170.2-1989 (Standards Australia 1989). The friction velocity (u_*) and the simulated roughness (z_o) height calculated from the velocity profile are 0.72 m/s and 0.23m respectively in full scale. Fig. 4(c) shows the non-dimensional longitudinal velocity spectra measured at the ridge height of the building along with the fitted Von Karman spectra due to ESDU (1974). The measured integral length scale of 0.248 m in the wind tunnel (equivalent to 24.8 m in full scale) at the building ridge height is found to be much lower than its target value of 54 m due to the constraints posed by the tunnel walls. While this would result in lower peak external pressures in the wind tunnel in comparison to the full-scale measurements, the dynamic response of internal pressure will however be affected to a much lesser extent.

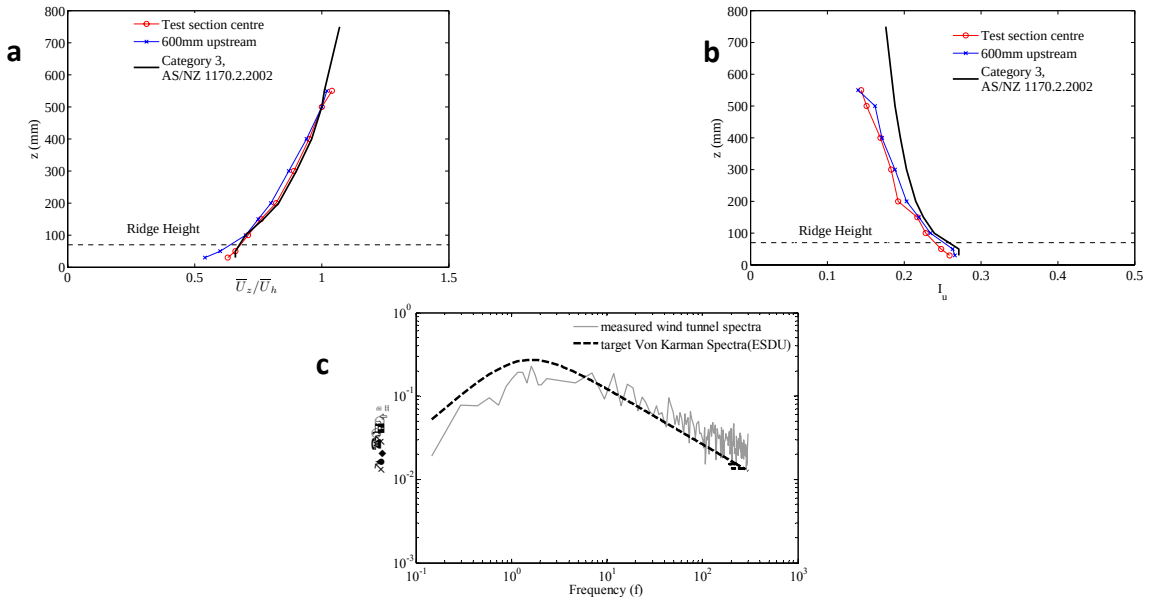

Fig. 4 Simulated boundary layer characteristics (a) velocity (b) turbulence intensity and (c) spectrum of longitudinal turbulence

The normalized frequency dependent admittance function of external windward opening and roof pressure coefficient fluctuations with respect to the ridge height dynamic pressure was estimated from the cross-spectrum measurements as

$$\left|\chi_{eWq}(\omega)\right|^2 = \left(\frac{q}{\overline{C}_{peW}}\right)^2 \frac{\left|S_{C_{peW}q}(\omega)\right|}{S_q(\omega)} \tag{25a}$$

$$\left|\chi_{rq}(\omega)\right|^2 = \left(\frac{q}{\overline{C}_{pr}}\right)^2 \frac{\left|S_{C_{pr}q}(\omega)\right|}{S_q(\omega)} \tag{25b}$$

where $S_{CpeWq}(\omega)$ and where $S_{Cprq}(\omega)$ are the cross-spectral density of the windward wall and roof external pressure with the ridge height dynamic pressure respectively. This was done to eliminate the un-correlated noise in the signals. 34 blocks of 1024 consecutive data samples were used to calculate the average spectra in each case. The phase function as obtained from cross-spectral density [$S_{CpeWCpr}(\omega)$] between the windward wall and the roof external pressure is given by

$$\varphi_{eWr}(\omega) = \arg\left[S_{C_{peW}C_{pr}}(\omega)\right] \tag{26}$$

The results for external windward and roof pressure admittance and phase functions, obtained from the wind tunnel measurements, plotted against reduced frequency are presented in Figs. 5(a) and (b) respectively.

While the windward wall pressure admittance function $|\chi_{eWq}|^2$ shows attenuation in the high frequency region, the high frequency fluctuations observed for the roof pressure admittance function $|\chi_{rq}|^2$ is probably due to intermittent turbulence generated in the shear layer due to separation at the windward edge. The phase function shows a value of 180° or π radian at the lower frequencies but tends towards 0° at higher frequencies. These relationships were further used for calculation of internal and net pressure admittance functions $|\chi_{iq}|^2$ and $|\chi_{nq}|^2$ and spectra for different combinations of roof flexibility and background leakage for the TWFT building with a dominant windward opening.

5. Comparison between theoretical predictions and wind tunnel results

In order to validate the theoretical predictions, wind tunnel tests using the physical model described in the previous section along with a flexible Styrofoam roof of mass (m_r) 20 g and area (A_r) 0.112 m^2 were carried out (see Fig. 6). The natural frequency of the flexible roof under boundary conditions similar to its attachment to the model was estimated to be around 99 Hz using

forced vibration tests involving laser vibro-meter (Polytec OFV 056) measurements. This was found to be approximately 6.6 times higher than the theoretical undamped Helmholtz frequency (f'_{HH}) of around 15 Hz, of the cavity model with the flexible roof and full-scale opening area of 5m by 4.2 m. The roof can therefore, be considered to be quasi-statically flexible as per standard definition. The value of b for the Styrofoam roof based on its pneumatic stiffness against the sealed model was estimated to be approximately 2.57. It is worth noting that a match between the theoretical and measured Helmholtz frequency was obtained by using a flow contraction coefficient (c) of approximately 0.6, resulting in a net effective air slug length (l_{eW}) of $l_{eW} = 1.48\sqrt{A_W}$. This is within the range of the net effective slug length of 1.1-1.63$\sqrt{A_0}$, experimentally obtained by Sharma *et al.* (2010) for openings at different locations on the windward wall. 80 leakage holes each of diameter 2.5 mm were distributed uniformly on the leeward and side walls of the model. The leakages could be blocked-off in any combination to modify the building porosity. Porosity ratios of 0, 10 and 20% for a windward wall opening area of 5 cm by 4.2 cm were tested in the wind tunnel for comparison with analytical predictions. Theoretical predictions involved usage of loss coefficient C_{LW}= 1.2 for the dominant opening and $\overline{K}_L$ =2.78 for the lumped leakage.

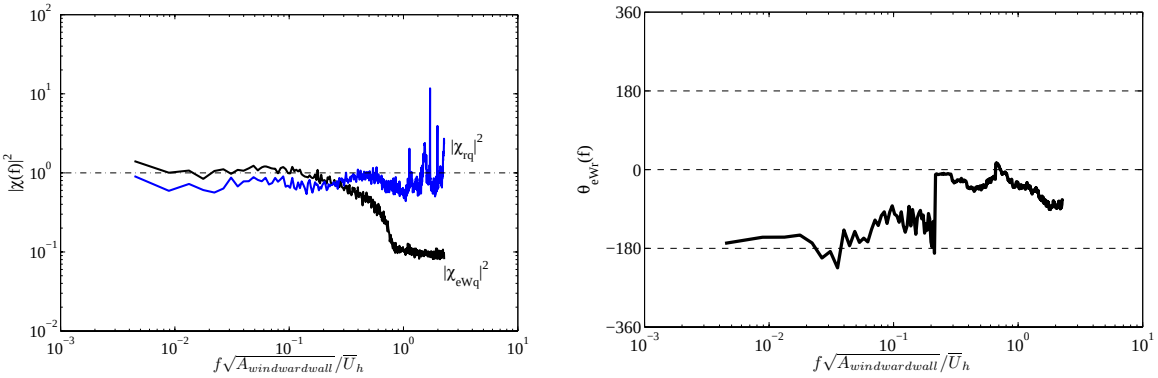

(a) (b)

Fig. 5 (a) Admittance functions $|\chi_{eWq}|^2$ and $|\chi_{rq}|^2$ and (b) phase function φ_{eWr}

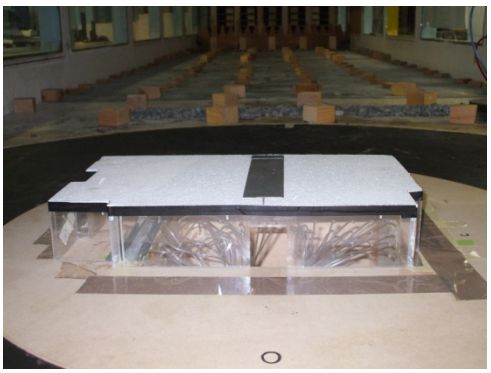

Fig. 6 Model with a flexible Styrofoam roof inside the de Bray wind tunnel

An appropriate value of C_{LW} is open to argument with Oh *et al.* (2007) and Holmes and Ginger

(2012) providing a review of the values reported in literature. While the reported values show a widespread scatter, Ginger *et al.* (2010), based on experimental investigations, have recently argued that the value of C_{LW} is a function of the building volume-opening area and wind speed. Values of C_{LW} as high as 100 were obtained for buildings with smaller volumes and comparatively larger opening areas. However, such high values, in addition to the inclusion of the losses through the opening, also suggest the possibility that the measured loss coefficients were affected with the damping influence of leakage and skin flexibility inherently present in the experimental models. The value of C_{LW}= 1.2 used in this study, on the other hand, has been computationally obtained by Sharma and Richards (1997a,c) by modelling the losses through the opening in isolation for a rigid, non-porous TTU building. Additional experiments were also carried out to validate this computational prediction. Chaplin *et al.* (2000) further reported values of C_L similar or very close to those being used here and by Sharma and Richards (1997a,c) from their idealized wind tunnel measurements. A value of $\overline{K}_L$ =2.78 used herein is close to those being reported by Vickery (1986), Yu *et al.* (2008) and Guha *et al.* (2011) based on theoretical and wind tunnel investigations.

Fig. 7(a) shows the internal pressure to windward wall pressure admittance functions $|\chi_{ieW}|^2$ plotted against frequency for different leakage to dominant opening area ratios obtained theoretically while Fig. 7(b) shows the admittance functions obtained from wind tunnel measurements for the corresponding building porosities. It should be noted the measured admittance functions were obtained from cross-spectral estimates between the windward wall external and internal pressure signals. While the match between theory and measurements is reasonable in the low-frequency range, the magnitude of the measured admittance at resonance is lower compared to the theoretical predictions for all building porosities. This is possibly due to the compliance of the wind tunnel model walls and the volume chamber as well as leakage in the Styrofoam roof not accounted for in the theoretical analysis. The measured admittance functions also show some evidence of high frequency noise well beyond 150 Hz in the system. The increased damping at resonance with increase in building porosity, as theoretically predicted, is also evident from measurements.

Figs. 8(a) and (b) similarly show the internal pressure to roof external pressure admittance functions $|\chi_{ir}|^2$ obtained theoretically and from wind tunnel measurements respectively. Again the agreement is satisfactory in the low frequency region; however the influence of background porosity in limiting the resonant response of internal pressure is more distinct in the measured admittance compared to the analytical prediction. The magnitude of the measured admittance function at resonance is slightly higher than the theoretical predictions for all building porosities. This is opposite to what was observed for the internal to windward wall pressure admittance functions in Figs. 7(a) and (b).

The predicted spectra of internal pressure coefficient for the flexible-roofed model with different porosities are plotted in Fig. 9(a) along with the measured spectra in Fig. 9(c). Also plotted in Figs. 9(a) and (c) are the spectra of the measured external pressure coefficient near the opening. Fig. 9(c) additionally shows the corresponding internal pressure coefficient for the rigid acrylic roof model tested for comparison. The low-frequency shift in the resonant peak for the flexible-roofed model due to the corresponding decrease in the Helmholtz frequency (≈15 Hz) compared to that of the rigid-roofed model (≈33 Hz) is evident from measurements. The response of internal pressure at the Helmholtz frequency of model is also found to decrease with increase in building porosity in both the predicted and the measured spectra. The internal pressure spectra in

both Figs. 9(a) and (c) also show high frequency fluctuations beyond 100Hz transmitted through the flexible roof. Similar phenomena is however, not observed in the windward wall external pressure spectrum.

Figs. 9(b) and (d) are the close up of Figs. 9(a) and (c) respectively near the Helmholtz frequency of the building model. The theoretical spectra simulated using a loss coefficient (C_{LW}) of 1.2 exhibits a slightly higher response compared to the measured spectra for all building porosities.

A better match between the measured and the predicted spectrum is obtained using a loss coefficient value of 6.9 compared to the value of 1.2, as shown in Fig. 9(e) for the flexible non-porous (r=0%) model. As discussed earlier, compliance of the wind tunnel model walls of thickness 6mm (including large panels used to assemble the volume chamber for scaling) and the inherent leakage on the flexible Styrofoam roof, not accounted for separately in the theoretical analysis, may possibly be responsible for the apparent increase in the loss coefficient (C_L); hence a higher loss coefficient value needed to effect the match. Therefore, an experimentally validated value of C_{LW}=1.2 (Sharma and Richards 1997a,c, Chaplin *et al.*, 2000) that accounts for only the losses through the opening, as should be the case, was subsequently used for numerical analysis.

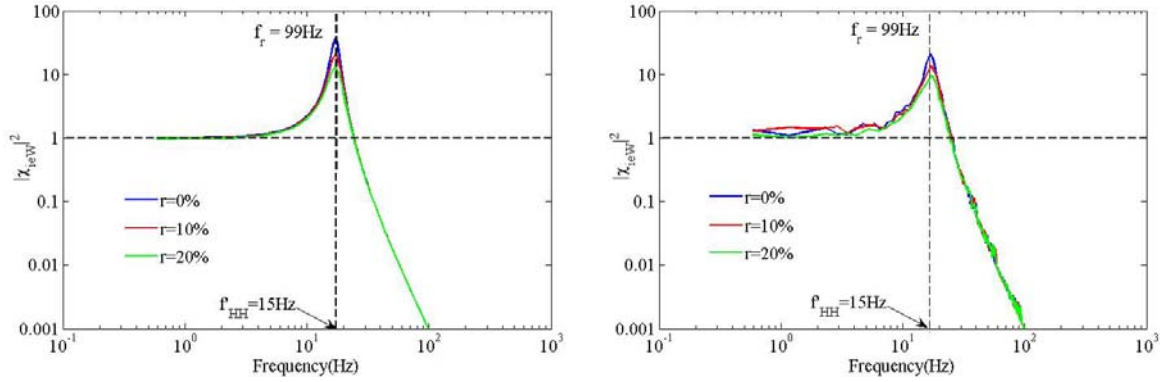

(a) (b)

Fig. 7 Admittance function $|\chi_{ieW}|^2$ for a flexible-roofed building with different porosities (a) theoretical and (b) wind tunnel

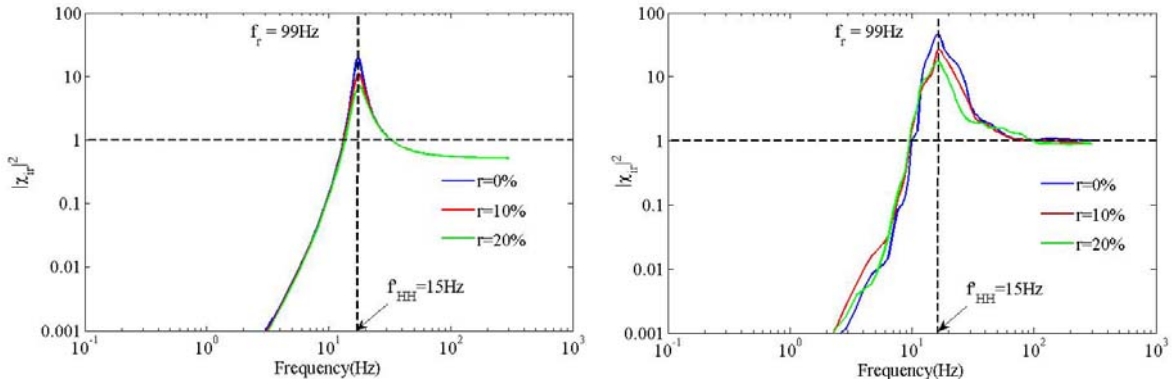

(a) (b)

Fig. 8 Admittance function |χir|2 for a flexible-roofed building with different porosities (a) theoretical and (b) wind tunnel

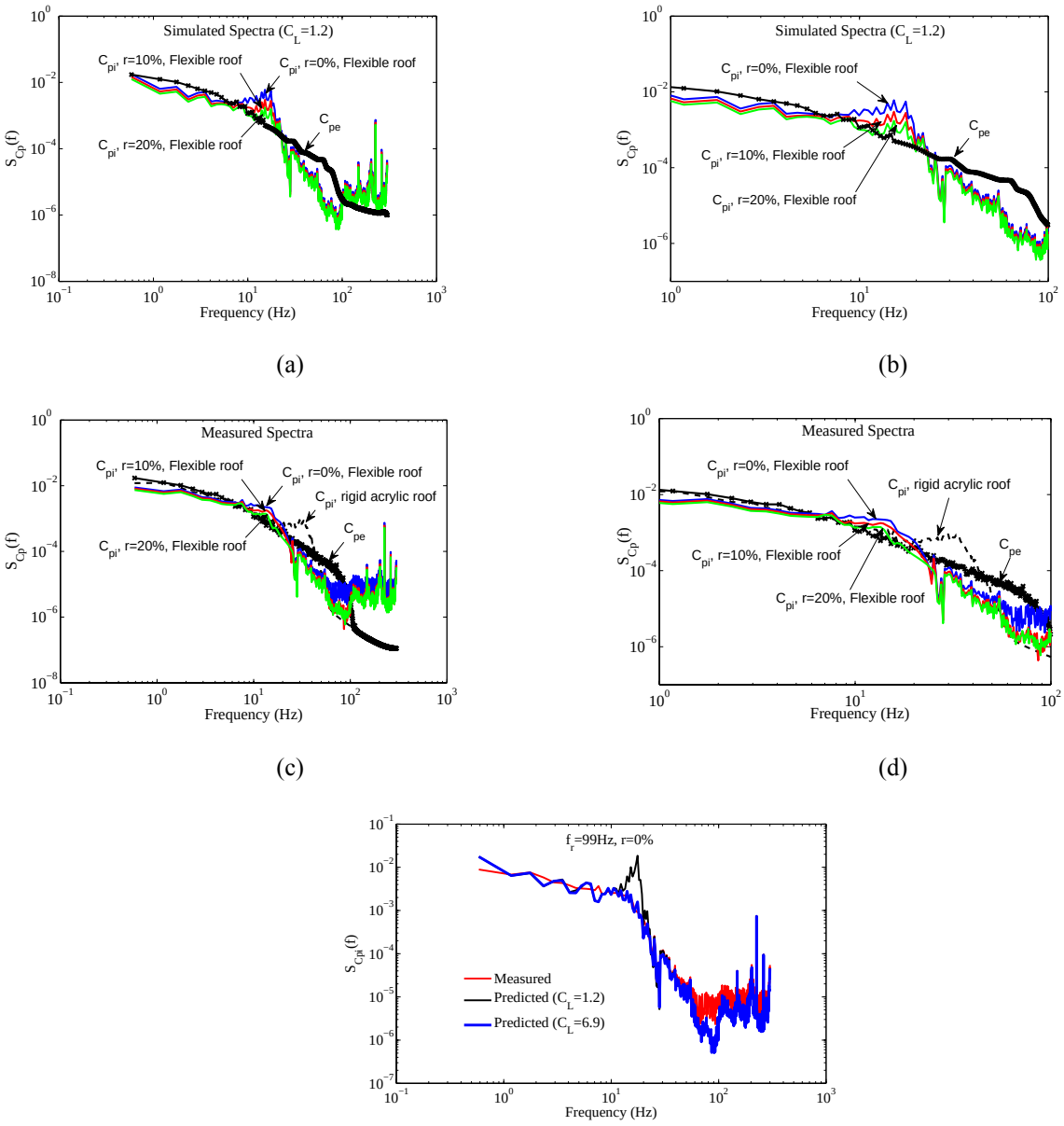

Fig. 9 Internal pressure coefficient spectra for a flexible-roofed building with different porosities (a) theoretical (b) close up of 9(a), (c) wind tunnel (d) close up of 9(c) and (e) Sensitivity of the predicted internal pressure spectra with CL for comparison with measurements

6. Numerical analysis and discussions

Having shown that the theory matches the experimental predictions, at least in terms of predicting the nature of transfer functions at or below the Helmholtz frequency of the system, numerical studies of the internal and net fluctuating pressure response were carried out for a prototype full scale building. In particular, a building similar in dimensions to the TFWT building, with the following parameters was considered.

$V_0 = 6.18\text{x}10^3\ \text{m}^3$, $A_W = 21\ \text{m}^2$, $A_r = 874\ \text{m}^2$,
$l_{eW} = 1.48\sqrt{A_W}$, $C_{LW} = 1.2$, $\overline{U}_h = 30\text{m/s}$, $\rho_a = 1.185\text{kg/m}^3$,
$\gamma = 1.4$, $P_a = 101300\text{Pa}$, $\overline{C}_{pi} \approx \overline{C}_{peW} = 0.7$, $\widetilde{C}_{peW} = 0.25$, $\overline{C}_{pr} = -0.65$, $\widetilde{C}_{pr} = 0.17$;
$\overline{C}_{peL} = -0.1$, $\overline{K}_L = 2.78$, $I_u = 0.20$

Some of these parameters such as the mean and root-mean-squared windward and roof external pressure, mean leeward wall external pressure, ridge height turbulence intensity as well as the admittance and phase functions of the windward and roof external pressures to the ridge height dynamic pressure, [$|\chi_{eWq}|^2$, $|\chi_{rq}|^2$ and φ_{eWr}] were obtained from the wind tunnel experiments. The internal to windward wall external and roof pressure admittance and phase functions, $|\chi_{ieW}|^2$, $|\chi_{ir}|^2$, φ_{ieW} and φ_{ir}, were estimated analytically using Eqs. (21) and (22). The internal and net roof pressure to the ridge height dynamic pressure admittance functions, $|\chi_{iq}|^2$ and $|\chi_{nq}|^2$, as well as the spectra of internal and net roof pressures for different flexibility-leakage combinations were evaluated using these measured and analytically estimated admittance functions as per Eqs. (23) and (24).

Values of b, for roof structural frequencies of 5 and 10 Hz and mass 15 tonnes, are estimated as 1.2 and 0.3 respectively. The Helmholtz frequency (f'_{HH}) for the building with these flexible envelopes calculated using Eq. (14) is 0.84 Hz and 1.09Hz against that for the rigid building of frequency (f_{HH}) = 1.25 Hz. The critical leakage frequency (f_c) calculated using Eq. (18) for leakage to dominant opening area ratios (r) of 0, 10% and 20% used in the study are 0, 0.06 and 0.11 Hz respectively for b = 1.2; and 0, 0.10 and 0.19 Hz respectively for b = 0.3. The critical leakage frequencies are usually found to be an order of magnitude smaller than the corresponding Helmholtz frequency of the building with the dominant opening (Vickery 1986). The damping coefficient (c_{j1}) given by Eq. (20) for each leakage-envelope flexibility combination is calculated using a "detailed" iterative procedure explained in Yu *et al.* (2006).

Figs. 10(a) and (b) compares the admittance functions of internal to windward external pressure $|\chi_{ieW}|^2$ for different leakage to dominant opening ratios for roof structural frequencies 5 and 10 Hz respectively plotted against the reduced frequency. The damping effect of the leakage at resonance is evident in these figures. The effect of quasi-static flexibility is indicated by a low-frequency shift in the resonant peak in Fig. 10(c) due to the corresponding decrease in the Helmholtz frequency for the roof with structural frequency 5 Hz compared to that for the 10 Hz roof. The associated reduction in admittance level for the 5Hz roof at the resonant peak indicates an increase in magnitude of damping in the system contributed by the more compliant roof.

Figs. 11(a) and (b) similarly compare the admittance functions of internal to roof external pressure $|\chi_{ir}|^2$ for different leakage combinations for the 5 and 10 Hz roof respectively. The

admittance is found to be unity beyond the Helmholtz frequency of the system; meaning that the roof external pressure fluctuations due to body generated turbulence will increase the strength of the internal and net roof pressure admittances at higher frequencies.

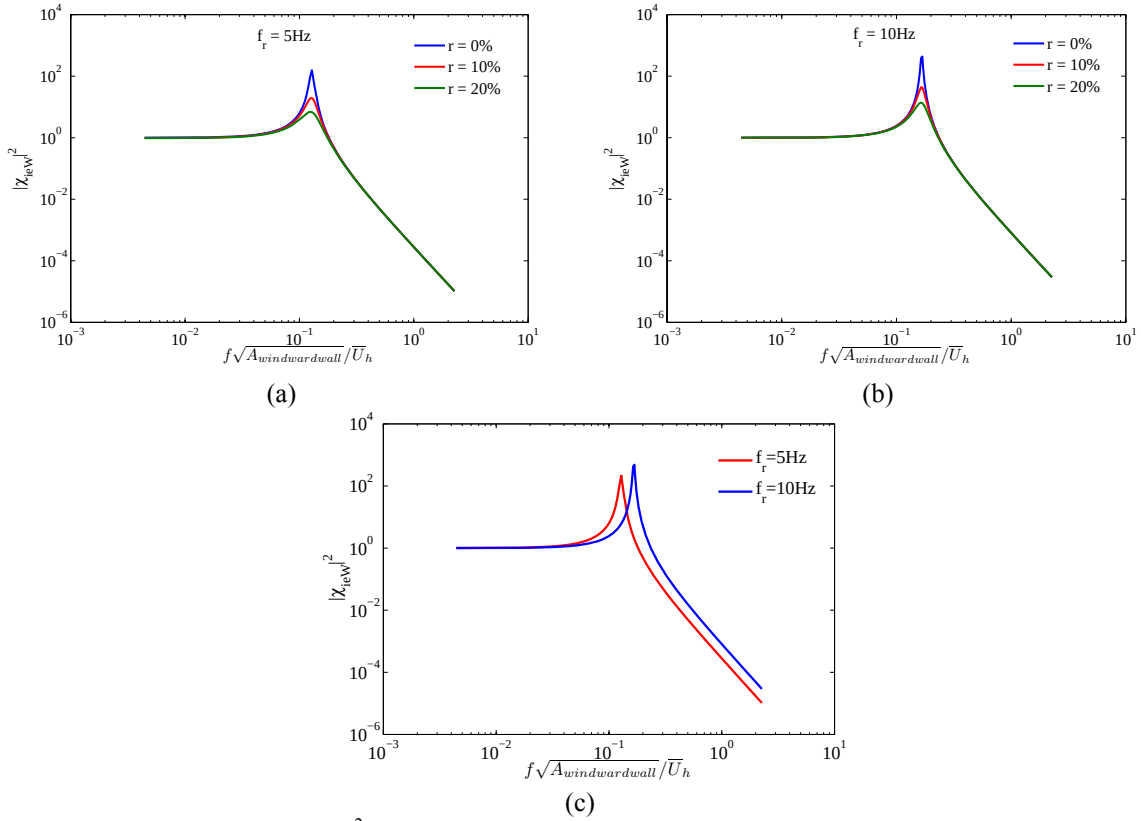

(a) (b)

(c)

Fig. 10 Admittance function $|\chi_{ieW}|^2$ for different leakage ratios for the building with roof structural frequency (a) 5 Hz and (b) 10 Hz (c) Admittance function $|\chi_{ieW}|^2$ for 5 and 10 Hz roof with a non-porous (r=0%) envelope

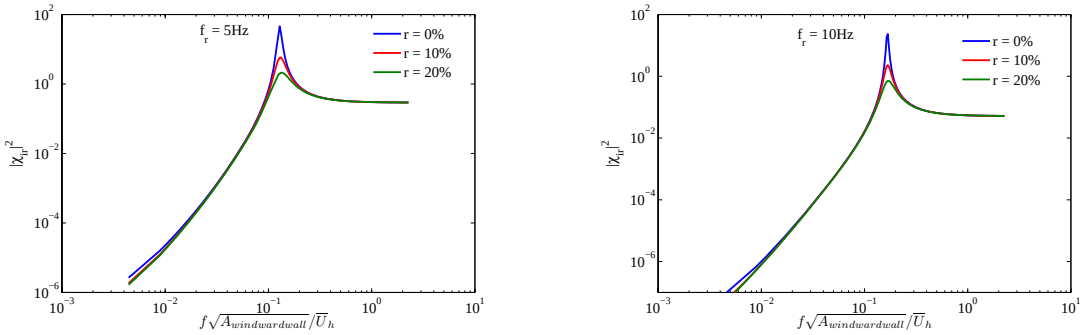

(a) (b)

Fig. 11 Admittance function $|\chi_{ir}|^2$ for different leakage ratios for the building with roof structural frequency (a) 5 Hz and (b) 10 Hz

Figs. 12(a) and (b) show the internal pressure admittance functions calculated using Eq. (23) for different leakage ratios for the 5 and 10 Hz roof respectively. The admittance of external windward and roof pressure fluctuations to the ridge height dynamic pressure and the phase relation between the windward and the roof pressure fluctuations used in the analyses were taken as those measured in the wind tunnel [Figs. 5(a) and (b)], the frequency being scaled through equality of reduced frequency between the model and full scale. While the admittance at resonance, for a given building porosity, is lower for the 5Hz compared to that for the 10 Hz roof, increase in background porosity, for a given roof, is found to further damp out the internal pressure fluctuations.

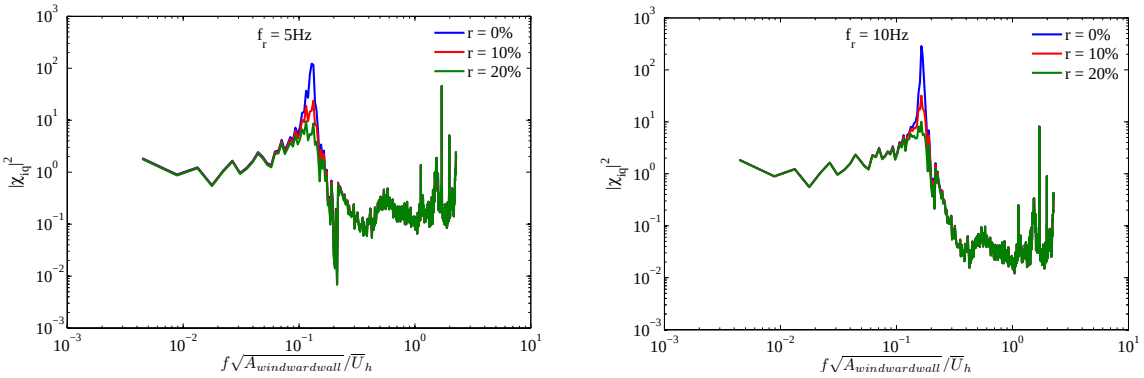

(a) (b)

Fig. 12 Internal pressure to ridge height dynamic pressure admittance functions $|\chi_{iq}|^2$ for different leakage ratios for the building with roof structural frequency (a) 5 Hz and (b) 10 Hz

The decrease in the Helmholtz frequency of the building due to increased envelope flexibility as evident in Figs. 10, 11 and 12 appears to be of significant consequence apparently due to the close proximity of the resulting resonant frequency to the energy containing frequencies of the turbulent external pressure fluctuations. Sharma and Richards (1997b) for example, have previously argued that the potential significance of this decreased Helmholtz frequency is a corresponding amplification of the internal pressure resonant response by around 2.5~3.

The situation could be even worse during tropical cyclone conditions, with inherent shift of the turbulence energy towards higher frequencies, resulting in a resonant response as high as 60 times the neutral atmospheric boundary conditions. The inclusion of the effect of background porosity of r =20% in the current study shows a corresponding reduction of the internal pressure gain at resonance by as much as 4.5~5.5 times as illustrated in Fig. 12. This reduction in the gain thus nullifies the possibility of such a dramatic increase.

Figs. 13(a) and (b) similarly shows the net roof pressure coefficient admittance functions for the 5 Hz and 10 Hz roof respectively. The effect of enhanced roof pressure admittances at higher frequencies results in building generated turbulence to be transmitted to the dynamic internal pressure system. This in combination with high suction roof pressure can then exacerbate the net roof pressure in buildings.

Figs. 14(a) and (b) shows the spectra of the internal and the net roof pressure coefficient for the 5 Hz roof while Figs. 14(c) and (d) shows the corresponding spectral counterparts for the 10 Hz

roof. Also shown in the spectral plots is the spectrum of the ridge height dynamic pressure. The plots reinforce the moderating effect of background leakage and higher envelope flexibility on the resonance of internal pressure in buildings. The RMS values for the fluctuating internal and net roof pressure coefficients obtained by numerical integration of the corresponding spectral curves for the different leakage-envelope flexibility combination is summarized in Table 1.

The RMS value of internal and net pressure progressively decreases with increase in background leakage and envelope flexibility. The effect of flexibility at higher leakage ratios (r = 20%) in the study is not obvious though, being dominated by the damping effect of leakages. The RMS internal and net roof pressure coefficients for a building with a flexible roof of structural frequency 5Hz and porosity ratio of 20% is found to be approximately 41 and 14.3% lower than that of a nominally sealed building with a dominant opening and rigid roof.

The significance of the transmission of the roof envelope external pressure fluctuations to the building interior and the net load on the building roof is exhibited through estimation of the correlation coefficient between the computed internal pressure and the roof pressure for various envelope flexibility-leakage combinations summarized in Table 2.

A high anti-correlation upwards of 0.53 exists between the roof external and internal pressures signifying the possibility of increased net loads on the roof surface. The correlations however increase with increase in envelope flexibility and background leakage, thus nullifying the damping effect of envelope flexibility and leakage to some extent.

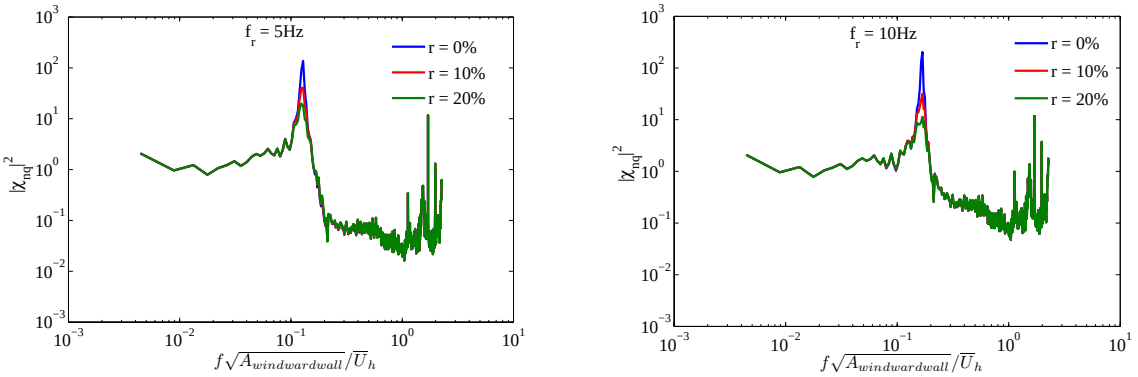

(a) (b)

Fig. 13 Net roof pressure to ridge height dynamic pressure admittance functions $|\chi_{nq}|^2$ for different leakage ratios for the building with roof structural frequency (a) 5 Hz and (b) 10 Hz

Table 1 Calculated RMS internal and net pressure coefficients

f_r (Hz)	$\widetilde{C}_{pi}$			$\widetilde{C}_{pn}$		
	r=0%	r=10%	r=20%	r=0%	r=10%	r=20%
5	0.20	0.15	0.13	0.33	0.31	0.30
10	0.21	0.16	0.14	0.34	0.31	0.30
Inf (Rigid)	0.22	0.16	0.14	0.35	0.31	0.30

Table 2 Calculated correlation coefficients between the roof and internal pressure

f_r (Hz)	ρ_{ir}		
	r=0%	r=10%	r=20%
5	-0.61	-0.79	-0.87
10	-0.57	-0.77	-0.84
Inf (Rigid)	-0.53	-0.76	-0.83

7. Calculation of peak internal pressure: comparison with quasi-steady approach

A comparison between the peak internal pressure predicted by the theoretical model for compliant and porous envelopes to the quasi-steady predictions for a rigid, non-porous envelope of the same internal volume and dominant opening size is presented here. The Twisted Flow Wind Tunnel (TFWT) building used for numerical analysis in the preceding section is considered for the comparative study.

The peak internal pressure coefficient ($\hat{C}_{pi}$) is calculated from its mean and predicted r.m.s. values using the following relation

$$\hat{C}_{pi} = \overline{C}_{pi} + g\widetilde{C}_{pi} \tag{27}$$

where g is the peak factor with values usually ranging from 3.5~3.7.

The mean internal pressure coefficient ($\overline{C}_{pi}$) for each dominant opening-leakage configuration is estimated as the area-weighted average of the external pressures near the dominant windward opening and the leeward wall using the expression

$$\overline{C}_{pi} = \frac{\overline{C}_{peW}}{\left[1+\left(A_L/A_W\right)^2\right]} + \frac{\overline{C}_{peL}}{\left[1+\left(A_W/A_L\right)^2\right]} \tag{28}$$

Mean internal pressures coefficients of 0.57, 0.56 and 0.54 are obtained for porosity ratios 0, 10 and 20% using $\overline{C}_{peW}$ and $\overline{C}_{peL}$ of 0.57 and -0.1 respectively. The r.m.s. internal pressure coefficients ($\widetilde{C}_{pi}$) for the different building flexibility and porosity are obtained from Table 1.

Table 3 Comparison of peak internal pressures: Theoretical vs. Quasi-steady

f_r (Hz)	$\hat{C}_{pi}$ (Theoretical)			$\hat{C}_{pi,QS}$ (Quasi-steady)
	r=0%	r=10%	r=20%	
5	1.31	1.12	1.03	
10	1.35	1.15	1.06	1.49
Inf (Rigid)	1.42	1.15	1.06	

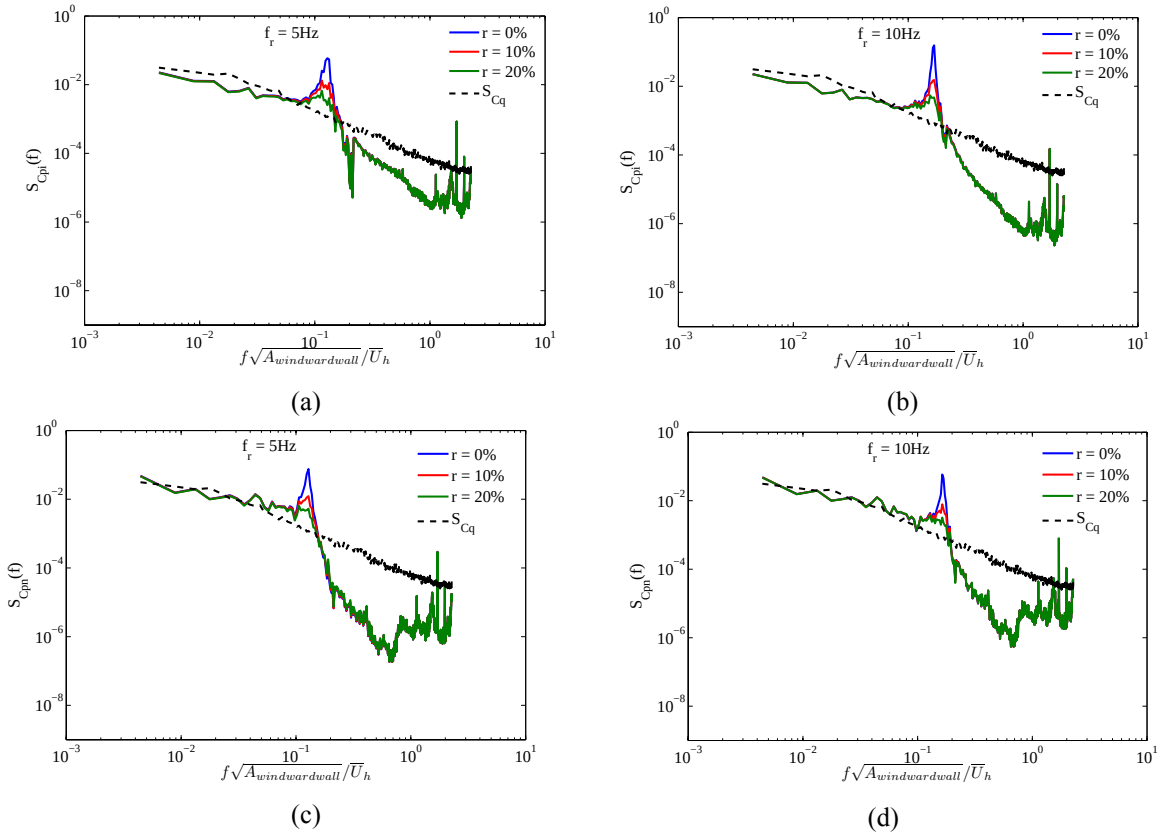

Fig. 14 (a) Internal pressure coefficient spectra (b) net roof pressure coefficient spectra for roof frequency 5Hz, (c) Internal pressure coefficient spectra (d) net roof pressure coefficient spectra for roof frequency 10Hz

The theoretically predicted peak internal pressure coefficients for different flexibility-leakage combinations are shown in Table 3. Also shown for comparison is the peak internal pressure coefficient obtained using quasi-steady analysis for a rigid non-porous building, where the mean external pressure coefficient ($\overline{C}_{peW} \approx 0.57$) and turbulent intensity ($I_u = 0.22$) measured in the wind tunnel is used for the estimation of the quasi-steady RMS internal pressure coefficient ($\widetilde{C}_{pi,QS}$) as

$$\widetilde{C}_{pi,QS} = 2\overline{C}_{peW} I_U \tag{29}$$

From Table 3, it is clear that the quasi-steady method, which does not take into account the effect of envelope compliance and background leakage, is conservative for all the flexibility-leakage combinations, but is close to the dynamic prediction for a rigid, non-porous envelope. In particular, the peak value of internal pressure coefficient for the building with 5 Hz roof and 20% porosity is around 31% lower than the peak pressure coefficient obtained using

quasi-steady analysis, thus exhibiting the enhanced damping due to envelope flexibility and background leakage.

8. Conclusions

An analytical model of internal pressure response of a leaky and quasi-statically flexible building with a dominant opening is provided. The influence of envelope external pressure fluctuations on the roof in addition to the fluctuating external pressure at the dominant opening has been included in the model to investigate the net fluctuating load on the envelope. A linearized version of the model is developed in particular, to establish the admittance functions of internal and net envelope roof pressure with respect to the onset turbulence. Wind tunnel experiments involving a flexible roof and different building porosities were carried out to validate the theoretical predictions. The agreement between theoretical and experimentally measured admittance functions of internal to windward and roof external pressure is found to be satisfactory; although an opening loss coefficient value of 1.2 used for theoretical analysis resulted in a slight over-prediction of the internal pressure resonant response. A better match between the experimental results and theoretical predictions is obtained using a loss coefficient value of 6.9.

The extent of the damping effects of "skin" flexibility and background leakage in moderating the internal pressure response under high wind conditions is shown using design examples involving a typical industrial warehouse. While the effect of envelope flexibility is shown to lower the Helmholtz frequency of the building volume-opening combination, the lowering of the resonant peak in the internal and net roof pressure coefficient spectra is attributed to the increased damping in the system due to inherent background leakage and flexibility in the envelope. A significant anti-correlation is however, found to exist between the internal and the roof external pressure fluctuations in all cases studied, thus exhibiting the possibility of increased net loads on the roof surface. The r.m.s. internal and net roof pressure coefficients for a building with a quasi-statically flexible roof of frequency 5 Hz and porosity ratio of 20%, are found to be approximately 40 and 15%, respectively, lower than those for a nominally sealed rigid building of the same volume and opening size. A comparison between the theoretically predicted peak internal pressure coefficients for different envelope flexibility-leakage combinations to that obtained using quasi-steady analysis for a rigid, non-porous building of the same internal volume and dominant opening size show over-prediction by the quasi-steady model. In particular, the peak internal pressure coefficient for a building with a 5 Hz flexible roof and 20% background porosity is found to be lower than the quasi-steady provisions by almost 31% in the current study. Previous research conducted with rigid, non-porous models has been used to criticize internal pressure provisions in wind loading standards; however the results of this study indicate that for real flexible and leaky buildings, the resonant response is much weaker and hence the criticism may be unwarranted.

References

Chaplin G.C., Randall, J.R., Baker, C.J. (2000), "The turbulent ventilation of a single opening enclosure", *J. Wind Eng. Ind. Aerod.*, **85**(2), 145-161.

Engineering Science Data Unit (1974), *Characteristics of atmospheric turbulence near the ground: Part 2-single point data for strong winds (neutral atmosphere)*, Data Item 74031, London, Engineering Science Data Unit.

Ginger, J.D., Holmes, J.D. and Kopp, G.A. (2008), "Effect of building volume and opening size on fluctuating internal pressures", *Wind Struct.*, **11**(5), 361-376.

Ginger, J.D., Holmes, J.D. and Kim, P.Y. (2010), "Variation of internal pressure with varying sizes of dominant openings and volumes", *J. Struct. Eng. - ASCE*, **136**(10), 1319-1326.

Guha, T.K., Sharma, R.N. and Richards, P.J. (2011), "Internal pressure dynamics of a leaky building with a dominant opening", *J. Wind Eng. Ind. Aerod.*, **99**(11), 1151-1161.

Halkyard, R., Blanchard, G., Flay, R.G. and Velychko, N. (2009), "Adaptation of tubing response correction filter coefficients to suit reduced sampling frequencies", *Proceedings of the 7th Asia-Pacific Conference on Wind Engineering*, Taipei, Taiwan.

Harris, R.I. (1990), "The propagation of internal pressures in buildings", *J. Wind Eng. Ind. Aerod.*, **34**(2), 169-184.

Holmes, J.D. (1979), "Mean and fluctuating pressure induced by wind", *Proceedings of the 5th International Conference on Wind Engineering*, Colorado State University, USA.

Holmes, J.D. and Ginger, J.D. (2012), "Internal pressures - the dominant windward opening case - a review", *J. Wind Eng. Ind. Aerod.*, accepted for publication.

Liu, H. and Saathoff, P.J. (1982), "Internal pressure and building safety", *J. Struct. Division*, **108**(10), 2223-2234.

Novak, M. and Kassem, M. (1990), "Experiments with free vibration of light roofs backed by cavities", *J. Wind Eng. Ind. Aerod.*, **116**(8), 1750-1763.

Oh, J.H., Kopp, G.A. and Inculet, D.R. (2007), "The UWO contribution to the NIST aerodynamic database for wind loads on low buildings: Part 3. Internal pressures", *J. Wind Eng. Ind. Aerod.*, **95**(8), 755-779.

Sharma, R.N. (1996), *The influence of internal pressure on wind loading under tropical cyclone conditions*, Ph.D. Thesis, The University of Auckland.

Sharma, R.N. (2008), "Internal and net envelope pressures in a building having quasi-static flexibility and a dominant opening", *J. Wind Eng. Ind. Aerod.*, **96**(6-7), 1074-1083.

Sharma, R.N. and Richards, P.J. (1997a), "Computational modelling of the transient response of building internal pressure to a sudden opening", *J. Wind Eng. Ind. Aerod.*, **72**, 149-161.

Sharma, R.N. and Richards, P.J. (1997b), "The effect of roof flexibility on internal pressure fluctuations", *J. Wind Eng. Ind. Aerod.*, **72**, 175-186.

Sharma, R.N. and Richards, P.J. (1997c), "Computational modelling in the prediction of building internal pressure gain functions", *J. Wind Eng. Ind. Aerod.*, **67-68**, 815-825.

Sharma, R.N. and Richards, P.J. (2003), "The influence of Helmholtz resonance on internal pressures in a low-rise building", *J. Wind Eng. Ind. Aerod.*, **91**(6), 807-828.

Sharma, R.N. and Richards, P.J. (2005), "Net pressures on the roof of a low-rise building with wall openings", *J. Wind Eng. Ind. Aerod.*, **93**(4), 267-291.

Sharma, R.N., Mason, S. and Philip, D. (2010), "Scaling methods for wind tunnel modelling of building internal pressures induced through openings", *Wind Struct.*, **13**(4), 363-374.

Standards Australia (1989), *SAA Loading Code. Part 2: Wind loads*. Standards Australia, North Sydney, New South Wales, Australia.

Standards Australia/Standards New Zealand (2002), *Structural design actions, Part2: Wind Actions.* Australian/New Zealand Standard AS/NZS 1170.2:2002, Standards Australia International Ltd., Sydney, and Standards New Zealand, Wellington, NZ.

Vickery, B.J. (1986), "Gust factors for internal pressures in low rise buildings", *J. Wind Eng. Ind. Aerod.*, **23**, 259-271.

Vickery, B.J. and Bloxham, C. (1992), "Internal pressure dynamics with a dominant opening", *J. Wind Eng. Ind. Aerod.*, **41**(1), 193-204.

Vickery, B.J. and Georgiou, P.N. (1991), "A simplified approach to the determination of the influence of internal pressure on the dynamics of large span roofs", *J. Wind Eng. Ind. Aerod.*, **38**(2-3), 357-369.

White F.M. (1999), *Fluid Mechanics*, 4th edition, McGraw-Hill, New York, USA.
Woods, A.R. and Blackmore, P.A. (1995), "The effect of dominant openings and porosity on internal pressures", *J. Wind Eng. Ind. Aerod.*, **57**(2-3), 167-177.
Yu, S.C. and Lou, W.J. (2006), "Wind-induced internal pressure fluctuations of structure with single windward opening", *J. Zhejiang University*, **7**(3), 415-423.
Yu, S.C., Lou, W.J. and Sun, B.N. (2008), "Wind-induced internal pressure response for structure with single windward opening and background leakage", *J. Zhejiang University*, **9**(3), 313-321.

Appendix

For the model shown in Figure 2 of a building with a flexible roof and leaky envelope, the internal pressure is forced by the turbulent external pressures transmitted through the dominant opening, roof and the background porosity in the walls.

For instantaneous displacements of x_W and x_L of air-slugs through the windward and leeward dominant opening and a roof displacement of x_r, the instantaneous volume (V) of air inside the building is given by

$$V = V_0 - A_W x_W + A_r x_r + A_L x_L \tag{A1}$$

where V_0 is the nominal volume of the building. Conservation of mass given by

$$0 = \rho_a \frac{dV}{dt} + V \frac{d\rho_a}{dt} \tag{A2}$$

where ρ_a is the density of air, requires the difference in the rate of mass influx and efflux at the opening to be equal to the rate of change of mass of air inside the building cavity. Substituting Eq. (A1) into the first term and invoking the isentropic gas law for air for the second term on the right-hand side of Eq. (A2) results in

$$\frac{\rho_a A_W \dot{x}_W - \rho_a A_L \dot{x}_L}{V_0} = \rho_a \frac{d\upsilon}{dt} + \upsilon \frac{q\rho_a}{\gamma P_a} \frac{dC_{pi}}{dt} \tag{A3}$$

where $\dot{x}_W$ is the velocity of air slug through the dominant opening, $\dot{x}_L$ is the velocity of flow through the lumped leakage and υ is the non-dimensional volume ratio given by

$$\upsilon = \frac{V}{V_o} = \frac{A_r\left(H_r + x_r\right)}{A_r H_r} = 1 + \frac{x_r}{H_r} \tag{A4}$$

where A_r and H_r are the area and height of the roof respectively. Assuming a quasi-steady flow, driven by the internal-external pressure difference through the lumped leakage, the velocity $\dot{x}_L$ is given by

$$\dot{x}_L = \sqrt{\frac{2q}{\overline{K}_L \rho_a} \left| C_{pi} - \overline{C}_{peL} \right|} \tag{A5}$$

where q is the ridge height dynamic pressure and $\overline{K}_L$ is the steady state loss coefficient through the lumped leakage. Substituting Eq. (A5) into Eq. (A3) results in an expression for the velocity of air slug through the dominant opening ($\dot{x}_W$)

$$\dot{x}_W = \frac{A_L}{A_W}\sqrt{\frac{2q}{\overline{K}_L\rho_a}\left|C_{pi}-\overline{C}_{peL}\right|}+\frac{qV_0}{\gamma P_a A_W}\upsilon\frac{dC_{pi}}{dt}+\frac{V_0}{A_W}\frac{d\upsilon}{dt} \tag{A6}$$

Differentiating Eq. (A6) with respect to time yields the acceleration ($\ddot{x}_W$) of the air slug

$$\dot{x}_W = \frac{A_L}{A_W}\sqrt{\frac{q}{2\overline{K}_L\rho_a\left|C_{pi}-\overline{C}_{peL}\right|}}\frac{dC_{pi}}{dt}+\frac{qV_0}{\gamma P_a A_W}\left(\upsilon\frac{d^2C_{pi}}{dt^2}+\frac{d\upsilon}{dt}\frac{dC_{pi}}{dt}\right)+\frac{V_0}{A_W}\frac{d^2\upsilon}{dt^2} \tag{A7}$$

Assuming air density changes to be small, the unsteady form of Bernoulli's equation through the windward dominant opening applied to a streamline connecting the immediate external region with external pressure coefficient $C_{peW}(t)$ to an internal point away from the opening with pressure coefficient $C_{pi}(t)$ can be written as

$$\rho_a l_{eW} A_W\ddot{x}_W+\frac{1}{2}\rho C_{LW}A_W\left|\dot{x}_W\right|\dot{x}_W = A_W q\left(C_{peW}-C_{pi}\right) \tag{A8}$$

where l_{eW} is the net effective length of the air slug and C_{LW} is the loss coefficient of flow through the opening. Substituting Eqs. (A6) and (A7) into Eq. (A8) results in the generalized model of internal pressure response for a porous building with dynamically flexible envelope. The resulting equation for $\upsilon \approx 1$ is given by

$$\begin{aligned}
&\underbrace{\frac{V_0\rho_a l_{eW}}{\gamma P_a A_W}\ddot{C}_{pi}}_{\text{Intertial Term}}+\underbrace{\frac{V_0\rho_a l_{eW}}{\gamma P_a A_W}\dot{\upsilon}\dot{C}_{pi}}_{\text{Interaction Damping Term}}+\underbrace{\frac{l_{eW}}{\overline{U}_h\sqrt{\overline{K}_L}}\left(\frac{A_L}{A_W}\right)\frac{\dot{C}_{pi}}{\sqrt{\left(C_{pi}-\overline{C}_{peL}\right)}}}_{\text{Pseudo-linear Damping Term}}+\frac{V_0\rho_a l_{eW}}{qA_W}\ddot{\upsilon}\\
&+C_{LW}\frac{V_0^2\rho_a q}{2\left(\gamma P_a A_W\right)^2}\left|\dot{C}_{pi}+\underbrace{\frac{2A_L\gamma P_a}{\rho_a\overline{U}_h V_0\sqrt{\overline{K}_L}}\left[\left(C_{pi}-\overline{C}_{peL}\right)\right]^{1/2}}_{\substack{\text{Additional damping}\\ \text{due to Leakage}}}+\underbrace{\frac{\gamma P_a}{q}\dot{\upsilon}}_{\substack{\text{Additional damping}\\ \text{due to Flexibility}}}\right|\\
&\underbrace{\left(\dot{C}_{pi}+\frac{2A_L\gamma P_a}{\rho_a\overline{U}_h V_0\sqrt{\overline{K}_L}}\left[\left(C_{pi}-\overline{C}_{peL}\right)\right]^{1/2}+\frac{\gamma P_a}{q}\dot{\upsilon}\right)}_{\text{Non-linear Damping Term}}\\
&=\underbrace{C_{peW}}_{\text{Forcing Function}}-\underbrace{C_{pi}}_{\text{Stiffness Term}}
\end{aligned} \tag{A9}$$

The inertial term in the equation determines the undamped Helmholtz frequency of the non-leaky rigid building. The interaction damping term arises out of the coupled interaction between the flexible envelope and internal pressure system. This is especially important for low-rise large-span multi-framed industrial buildings. The pseudo-linear damping term

incorporates the damping effect imparted by the background leakage and is proportional to the porosity ratio (A_L/A_W) of the building.

The non-linear damping term shows that in addition to the damping effects imparted by the losses through the opening (C_{LW}), wind speed (q) and the internal building volume (V_0), further (enhanced) damping is provided out of the complex interaction of the internal pressure with background leakage and envelope flexibility i.e., the additional terms due to leakage and flexibility in the non-linear damping term. For a rigid ($\upsilon = \dot{\upsilon} = \ddot{\upsilon} = 0$), non-porous building ($A_L = 0$), this term reduces to the usual non-linear damping term found in the established model(s) for internal pressure.